Broadband Optoacoustic Characterization of cMUT and PZT Transducer Directivity in Receive Mode

Johannes Rebling,[a,b] Omri Warshavski,[c] Cyril Meynier,[c] Daniel Razansky[a,b,*]
[a]Institute for Biological and Medical Imaging (IBMI), Helmholtz Center Munich, Ingoldstädter Landstraße 1, 85764 Neuherberg, Germany
[b]Faculty of Medicine, Technical University of Munich, Ismaninger Straße 22, 81675 Munich, Germany
[c]Advance Research Department, VERMON 180 Rue du General Renault 37038 Tours, France

ABSTRACT

Optoacoustic imaging is a rapidly developing area of biomedical imaging due its combination of rich optical contrast and ultrasound depth penetration. Just like conventional pulse-echo ultrasound imaging, optoacoustic tomography relies on the use of ultrasound detector arrays with a large number of elements. The precise knowledge of the transducer's sensitivity is crucial for the prediction of its performance for a given imaging task. Sensitivity characteristics such as the central frequency and bandwidth are routinely characterized. However, this characterization is typically performed solely under normal incidence since the measurement of the angle and frequency depended sensitivity (directivity) is difficult and time consuming with existing ultrasound characterization methods. We present a simple and fast characterization method for broadband directivity measurements of the angular transducer sensitivity based on the optoacoustic effect. The method utilizes a thin absorbing suture in order to generate omnidirectional and broadband optoacoustic signals, which are calibrated using a needle hydrophone. We applied this method to characterize and compare the directivity of a conventional piezoelectric (PZT) transducer to the directivity of a capacitive micromachined ultrasonic (cMUT) transducer. Both technologies showed a similar broadband response at normal incidence and the PZT transducer displayed a more than two times larger signal to noise ratio at normal incidence. However, the cMUT transducer's sensitivity was significantly less angle-depended and outperformed the PZT's sensitivity for angles larger than 20°.

Keywords: photoacoustic, directivity, ultrasound, spectrum, bandwidth, angle of incidence

1. INTRODUCTION

Optoacoustic (OA) tomographic imaging depends on the appropriate selection of ultrasound (US) detectors in order to accurately reconstruct the broadband responses generated in tissues[1–4]. Often, only the detector's sensitivity and bandwidth under normal incidence are considered when making this selection. However, the angle and frequency depended sensitivity (directivity) also plays an important role in enabling accurate reconstructions. Conventional US probes made from piezoelectric materials such as lead zirconate titanate (PZT) mainly emit and receive US waves under normal incidence, resulting in a good signal-to-noise (SNR) ratio in pulse-echo mode. However, this strong directivity is not a desirable characteristic for OA imaging systems as it results in limited-view image artifacts and reduces the overall resolution of the reconstructed images[2,5]. The precise knowledge of the transducer directivity is therefore required to make an informed decision about the transducer selection when building an imaging system. This directivity information can furthermore lead to a reduction in image artefacts in the OA image reconstruction, as it can help correct for the reduced sensitivity at larger angles, thus improving image quality and resolution. While piezocomposite transducers have dominated the US imaging field[6], the emerging technology of capacitive micromachined ultrasonic transducers (cMUT) has seen a rapid development in the last decade[7,8]. The possible integration of US transducer elements with amplifying and receiving electronics in one silicon chip hold great potential for highly sensitive yet affordable cMUT transducer arrays with thousands of elements. While such cMUT arrays

Medical Imaging 2017: Ultrasonic Imaging and Tomography, edited by Neb Duric, Brecht Heyde, Proc. of SPIE Vol. 10139, 101391K · © 2017 SPIE · CCC code: 1605-7422/17/$18 · doi: 10.1117/12.2253850

would be a great tool for both US and OA imaging, the development of cMUT arrays is costly and the characterization is difficult[9–12].

Here we introduced a calibrated optoacoustic characterization method for broadband directivity measurements of the angular transducer sensitivity. The method utilizes a simple absorbing suture in order to generate omnidirectional and broadband OA signals, which were characterized using a calibrated needle hydrophone. The calibrated optoacoustic source was used to compare the frequency dependence of the angular sensitivity of a conventional piezoelectric (PZT) and a capacitive micromachined ultrasonic (cMUT) transducer with similar size and central frequency.

2. METHODS

Figure 1 shows a schematic representation of the experimental setup used to characterize the transducers broadband directivity on the left in comparison to a conventional US characterization scheme shown on the right. In the presented system, the ultrasound directivity measurement relies on the generation of broadband ultrasound waves by the optoacoustic effect. At the heart of the setup is an optoacoustic line source, formed by a highly absorbing surgical suture with a 100 µm diameter and 4 mm length. In order to excite broadband OA signals, the suture was illuminated with short 16 mJ laser pulses. The directivity of an ultrasound transducer measures how sensitive the transducer is to plane waves incident under different angles. Conventional emit-receive directivity measurements employ a rotating ultrasound emitter in order to generate acoustic plane waves under different angles, as shown on the right in Fig. 1 whereas the presented method shown on the left of Fig. 1 measures the directivity using a simple linear translation of the tested transducer along one axis. As indicated in Fig. 1, the angle between the normal of the ultrasound wavefront and the normal of the transducer then only depends on the lateral position (along the y-axis) of the transducer. A complete directivity measurement was performed using a custom-made MATLAB script which controlled the laser, the linear stage as well as the data acquisition system. For each transducer position, several laser shots were triggered and a data acquisition system digitized and recorded the ultrasound time signals for each laser shot.

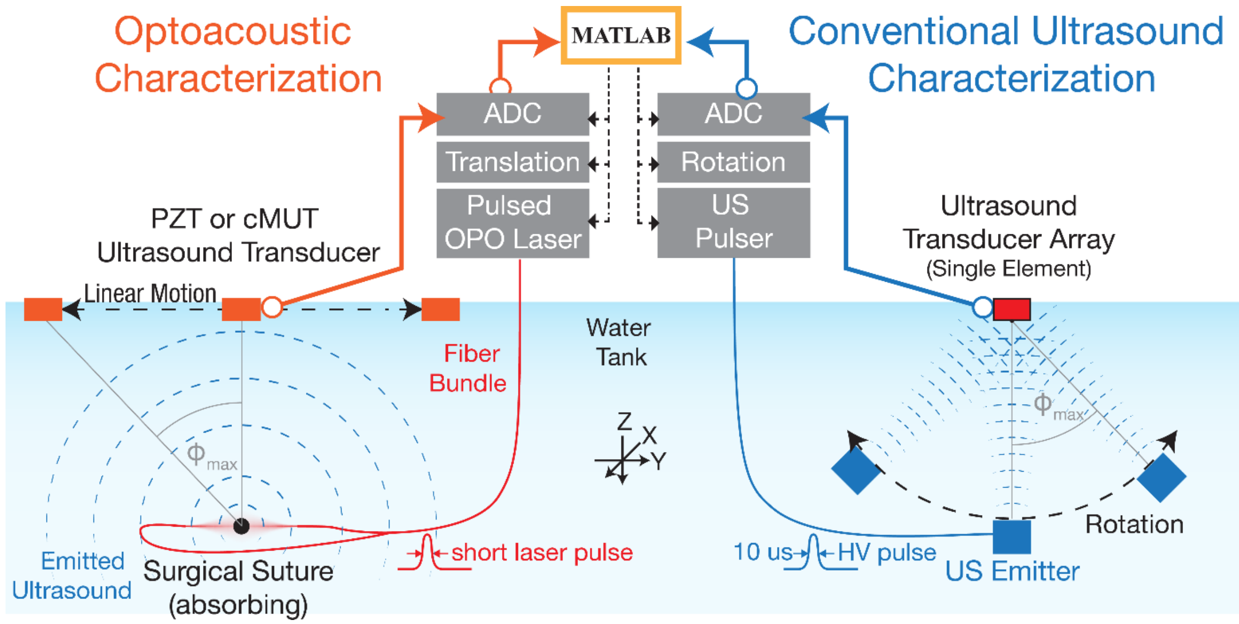

Figure 1. Illustration of the ultrasound transducer characterization based on the optoacoustic generation of broadband pulses shown on the left compared to conventional pulse-echo ultrasound characterization shown on the right.

The proposed characterization method was calibrated using a needle hydrophone. First, a calibrated PVdF needle hydrophone with a 1 mm diameter was used together with a matching wide-band amplifier and a DC coupler in order to characterize the broadband nature of the generated OA signals. The directivity measurement method proposed here is based on the assumption that the long surgical suture emits nearly ideal cylindrical waves when illuminated with pulsed laser radiation. To interrogate this assumption, we used a second PVdF needle hydrophone with a 75 µm diameter which we translated by means of the motorized linear stage. The 75 µm hydrophone has a very low directivity, performing almost like an idea point detector. To objectively compare the broadband directivity of conventional PZT transducers against the directivity of cMUT transducers, two linear arrays with almost identical geometry and similar central frequencies of approximately 5 MHz were characterized. The transducer sensitivity and directivity were then obtained by recording US time signals that were processed and analyzed using a custom-made MATLAB script.

3. RESULTS AND DISCUSSION

Figures 2a) and 2b) display the OA time signal and spectra of the surgical suture respectively. Figure 2a) shows the expected N-shaped OA response of a cylindrical source[13]. Figure 2b), calculated as the Fourier transform of the time signal in Fig 2a) demonstrates the broadband nature of the generated OA signals with a central frequency of approx. 5.5 MHz and an almost 150% -6 dB bandwidth of 8 MHz. Hence, the combination of 10 ns laser pulses and 100 µm diameter suture is well suited to characterize the directivity of transducers with a 5 MHz central frequency. The analysis of the 75 µm diameter hydrophone data (not shown) revealed a 6 dB decrease in OA signal amplitude over an angular range of ±40°, which is in good agreement with the literature for a hydrophone of that size[14], proving the omnidirectional nature of the emitted OA signals.

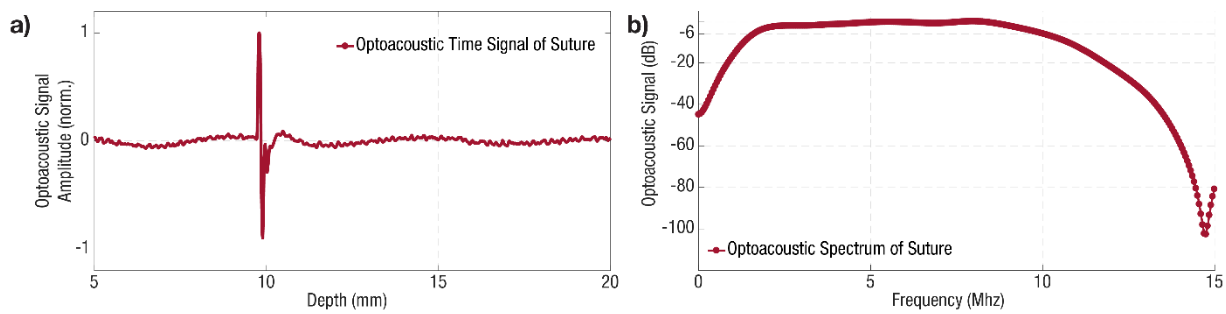

Figure 2. Optoacoustic signal emitted by a 100 µm diameter and 4 mm length surgical suture when illuminated with 10 ns laser pulses (16 mJ per pulse energy). a) Time signal converted to depth using the speed of sound, showing the characteristic symmetric, N-shaped optoacoustic response. b) Broadband OA spectrum emitted by the surgical suture, calculated as the Fourier transform of a).

Figure 3 shows both the PZT and cMUT transducer directivities based on the respective signal-to-noise ratios (SNR). Figures 3a) and 3b) display the depth signals recorded for different angles of incidence for the PZT and cMUT transducer respectively, with the cMUT transducer clearly recording signals at angles as high 55°. Figure 3c) display the absolute SNRs as a function of the incidence angle, indicating the favorable sensitivity of the PZT transducer (blue circles) at normal incidence with a maximum SNR of 266, more than twice that of the cMUT (orange dots) with a SNR of 108.

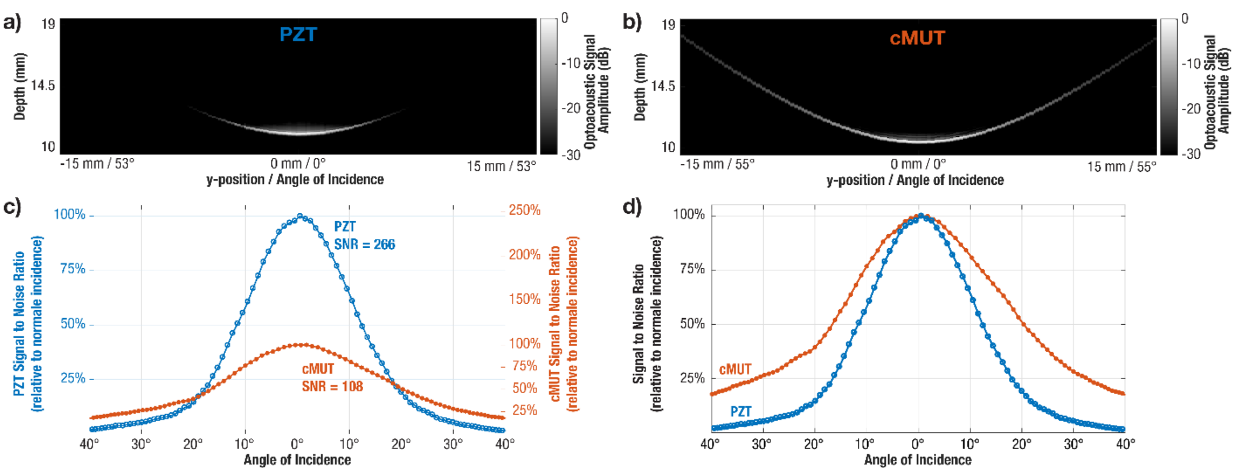

Figure 3. Comparison of PZT and cMUT transducer sensitivity characterized using the optoacoustic effect. Figures a) and b) show the sinogram, i.e. the depth signals recorded for different transducer positions and angles of incidence for the PZT and cMUT transducer respectively. Figures c) and d) display the signal-to-noise ratio (SNR) as a function of the incidence angle, with c) showing the absolute SNRs and d) showing the SNR relative to the maximum respectively. The PZT transducer has a favorable SNR at normal incidence as shown in c). However, the cMUT transducers shows a much less rapid decline in the SNR for larger angles of incidence and outperforms the PZT at angles higher than 20°.

Figure 3d) shows the SNRs relative to their respective maximum, where the cMUT demonstrates a much less rapid decline in the SNR for larger angles of incidence. Consequently, the cMUT outperforms the PZT and shows a large SNR at incidence angles higher than 20° as displayed in Fig. 3c).

The SNR based analysis shown Fig. 3 already provides important information regarding the angle-dependent sensitivity of both transducers. However, by applying the Fourier transform to the time signals shown in 3a) and b) one can obtain and analyze the angle and frequency depended sensitivity using the sensitivity maps shown in Figure 4. Figure 4a) shows the sensitivity maps of both the PZT (left) and the cMUT (right) transducers as a function of both angle and frequency. It is evident from these sensitivity maps, that the cMUT transducer shows a much broader angular sensitivity, especially in the frequency between 2 MHz and 6 MHz. While the sensitivity maps in Figures 4a) allow an intuitive and qualitative comparison of the transducer spectral sensitivity, Figures 4b) and 4c) enable an easier quantitative comparison of the PZT's (blue, dashed line) and cMUT's (orange, solid line) performance. Figure 4b) showcases the spectral sensitivity of both transducers for discrete angles of 0°, 20° and 40°. The sensitivity as a function of the frequency at normal incidence (0°, top in Fig. 4b) displays the characterization that is typically performed for US transducers. Both transducers show a similar broadband sensitivity with the cMUT's sensitivity shifted to slightly higher frequencies. A clearly advantageous performance of the cMUT transducer is observed for incidence angles of 20° and 40°, where the cMUT is significantly more sensitive over the entire frequency range. Similarly, Fig. 4c) showcases the angular sensitivity of both transducers for discrete frequencies of 3 MHz, 6 MHz and 9 MHz. The PZT's angular sensitivity varies little with Frequency and is reduced by almost 20 dB for angles of 20° and above. In contrast, the cMUT's sensitivity drops by only slightly more than 10 dB for angles as large as 45° at 3 MHz and 30° at 6 MHz. At 9 MHz the cMUT shows a similar decrease in sensitivity as the PZT while still outperforming the PZT's sensitivity for all angles.

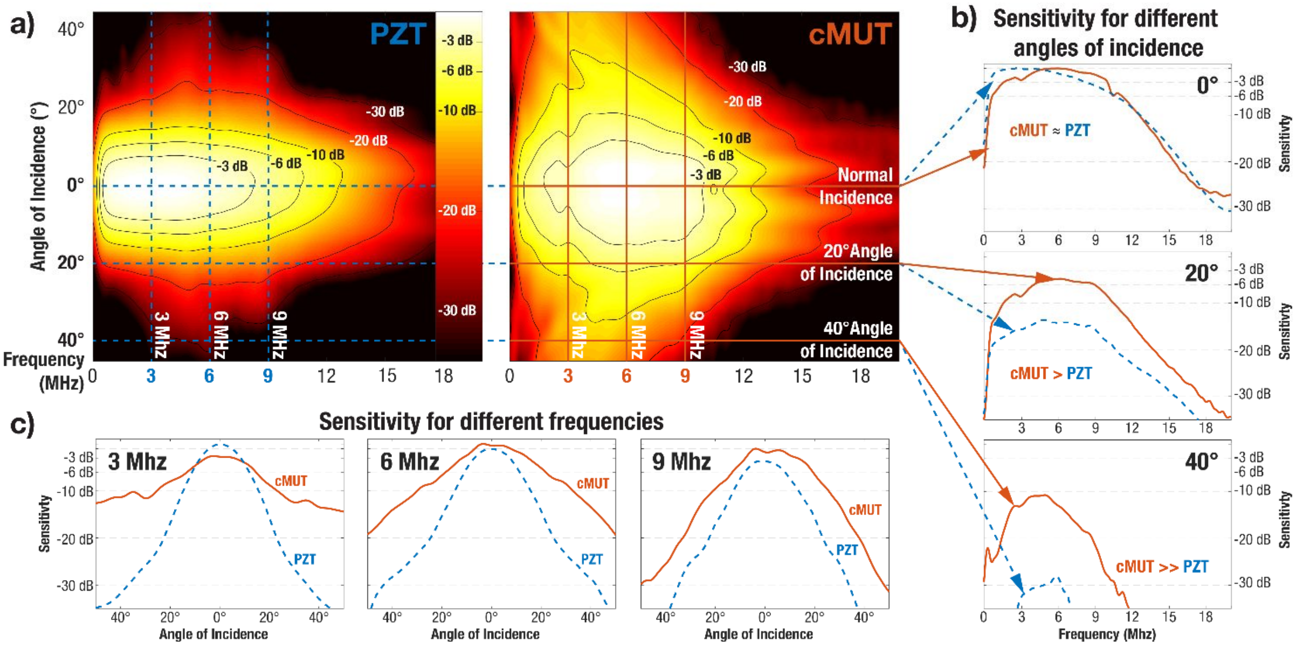

Figure 4. Frequency and angle dependent directivity characterization of PZT and cMUT transducers with an overview shown in a) and detailed quantitative comparisons shown in b) and c). a) Directivity maps of both the PZT (left) and cMUT (right) transducers with the directivity plotted as a function of both frequency (x-axis) and incidence angle (y-axis). b) Comparison of PZT (blue, dashed line) and cMUT (orange, solid line) sensitivity as function of the frequency for different incidence angles of 0°, 20° and 40°. c) Comparison of PZT (blue, dashed line) and cMUT (orange, solid line) sensitivity as function of the incidence angle for different frequencies of 3 MHz, 6 MHz and 9 MHz.

4. CONCLUSION

Here, we presented a methodology for accurate characterization of the broadband directivity of ultrasound transducers used in optoacoustic imaging systems. Our method allows the investigation of the transducers frequency response both under normal incidence as well as for arbitrary and large angles of incidence and with a flexible frequency range. The validity of the propose method was validated using calibrated hydrophones to both analyze the broadband nature of the emitted signals as well as to confirm their uniform propagation. We compared a conventional piezo-electric PZT transducer to a cMUT transducer with almost identical element geometries. The cMUT array showed a significantly larger angular sensitivity compared to the PZT transducer. The advantageous directivity of cMUT technology leads to fewer reconstruction artifacts, improving both the resolution and the signal to noise ratio of the reconstructed images. The directivity measurement can be adapted to the desired frequency range by changing the size of the line source, thereby changing the frequency of the emitted OA signals. No ultrasound emitter is required; the measurements are fast and simple, as they require no complicated alignment, and no additional hardware such as a rotation stage. The proposed method is readily applicable in existing OA tomography system and can help select the transducer best suited for OA imaging.

ACKNOWLEDGMENTS

The European Union through the OILTEBIA (Optical Imaging and Laser Techniques for Biomedical Applications) Grant (Agreement Number 317526) supported this work. The authors declare no conflicts of interest.

REFERENCES

[1] Rosenthal, A., Ntziachristos, V.., Razansky, D., "Acoustic Inversion in Optoacoustic Tomography: A Review.," Current medical imaging reviews **9**(4), 318–336 (2013).

[2] Lutzweiler, C.., Razansky, D., "Optoacoustic imaging and tomography: reconstruction approaches and outstanding challenges in image performance and quantification.," Sensors (Basel) **13**(6), 7345–7384 (2013).

[3] Wang, L., Yao, J., Wang, L.., Yao, J., "A practical guide to photoacoustic tomography in the life sciences," Nature Methods **13**, 627–638, Nature Methods (2016).

[4] Beard, P., "Biomedical photoacoustic imaging," Interface Focus **1**(4), 602–631, highwire (2011).

[5] Buehler, A., Rosenthal, A., Jetzfellner, T., Dima, A., Razansky, D.., Ntziachristos, V., "Model-based optoacoustic inversions with incomplete projection data.," Medical physics **38**(3), 1694–1704 (2011).

[6] Brown., "Design considerations for piezoelectric polymer ultrasound transducers," IEEE Transactions on Ultrasonics, Ferroelectrics and Frequency Control **47**(6), 1377–1396 (2000).

[7] Kshirsagar, A., Chee, R., Sampaleanu, A., Forbrich, A., Rishi, D., Moussa, W.., Zemp, R. J., "Multi-frequency CMUT arrays for imaging-therapy applications," Ultrasonics Symposium (IUS), 2013 IEEE International, 1991–1993, Ultrasonics Symposium (IUS), 2013 IEEE International (2013).

[8] Wygant, I., "A comparison of CMUTs and piezoelectric transducer elements for 2D medical imaging based on conventional simulation models," IEEE International Ultrasonics Symposium (IUS), 100–103, IEEE International Ultrasonics Symposium (IUS) (2011).

[9] Yang, T., Huang, D.., Wang, Y., "Directivity analysis of transducer array of acoustic directional dispersing device," International Conference on Mechatronics and Automation (ICMA), 2317–2321, International Conference on Mechatronics and Automation (ICMA) (2011).

[10] Conjusteau, A., Ermilov, S., Su, R., Brecht, H.-P., Fronheiser, M.., Oraevsky, A., "Measurement of the spectral directivity of optoacoustic and ultrasonic transducers with a laser ultrasonic source," Review of Scientific Instruments **80**(9), 093708 (2009).

[11] Bellared, F., Lardiès, J., Bourbon, G., Moal, P., Walter, V.., Berthillier, M., "Characterization of capacitive micromachined ultrasonic transducers," Microsyst Technol **22**(3), 593–601, springer (2016).

[12] Caliano, G., Carotenuto, R., Cianci, E., Foglietti, V., Caronti, A., Iula, A.., Pappalardo, M., "Design, fabrication and characterization of a capacitive micromachined ultrasonic probe for medical imaging.," IEEE transactions on ultrasonics, ferroelectrics, and frequency control **52**(12), 2259–2269 (2005).

[13] Wang, L., "Photoacoustic imaging and spectroscopy," CRC press (2009).

[14] Beard., Hurrell., Mills., "Characterization of a polymer film optical fiber hydrophone for use in the range 1 to 20 MHz: a comparison with PVDF needle and membrane hydrophones.," Ieee Transactions Ultrasonics Ferroelectr Freq Control **47**(1), 256–264, ieee (2000).